Ceramics International 47 (2021) 3741–3746

Contents lists available at ScienceDirect

Ceramics International

journal homepage: www.elsevier.com/locate/ceramint

Sintering behavior, phase structure and microwave dielectric properties of CeO_2 added $CaTiO_3$-$SmAlO_3$ ceramics prepared by reaction sintering method

Shicheng Zhou, Xiaowen Luan, Sang Hu, Xianjie Zhou, Sen He, Xi Wang, Hailin Zhang, Xiuli Chen, Huanfu Zhou *

Collaborative Innovation Centre for Exploration of Hidden Nonferrous Metal Deposits and Development of New Materials in Guangxi, Key Laboratory of Nonferrous Materials and New Processing Technology, Ministry of Education, School of Materials Science and Engineering, Guilin University of Technology, Guilin, 541004, China

ARTICLE INFO

Keywords:
$CaTiO_3$-$SmAlO_3$ ceramics
Reaction sintering method
Microwave dielectric properties

ABSTRACT

Novel 0.695$CaTiO_3$-0.305$SmAlO_3$+$x$wt% CeO_2 (x = 0, 0.5, 1.0, 1.5) ceramics were fabricated using a reaction-sintering (RS) approach. The crystal structure, morphology, and microwave dielectric properties of ceramics were systematically studied. The addition of CeO_2 could effectively improve the sintering behavior of 0.695$CaTiO_3$-0.305$SmAlO_3$ (CTSA) ceramics. When x = 0.5 wt%, the ceramics exhibited optimal microwave dielectric properties, with ε_r = 43.9, $Q\times f$ = 48 779 GHz, and τ_f = −0.24 ppm/°C, thereby indicating that the samples prepared via the RS route possess superior dielectric properties compared to those prepared by the conventional solid phase reaction. The results demonstrate that $CaTiO_3$-$SmAlO_3$ ceramics can be prepared simply and efficiently through a reaction-sintering process.

1. Introduction

The technical requirements of 5G networks have greatly increased the demand for key components in the communication system, such as filters, diplexers, and resonators. Microwave dielectric ceramics are key materials used in these devices. Because of the small size, light-weight quality, low loss, and low price of devices, microwave dielectric ceramics must meet the requirements of miniaturization, integration, high reliability, and low cost in communication technologies, such as mobile communication. Compared with other materials, such as metals and quartz crystals, microwave dielectric ceramics possess the advantages of low loss, high stability, and low thermal expansion coefficient. Therefore, the emergence of 5G communication technology has led to higher performance requirements for microwave dielectric ceramics [1–7].

Key performance requirements for microwave dielectric ceramics include a moderate dielectric constant (considering that a high dielectric constant can reduce the size and a low dielectric constant will reduce signal delay), low loss (suppression of signal damping), and near-zero τ_f value (to ensure thermal stability) [8–11]. However, in practical applications, high costs limit the application range of many microwave ceramics, such as $Ba(Zn_{1/3}Nb_{2/3})O_3$ and $Ba(Zn_{1/3}Ta_{2/3})O_3$ [12]. In order to satisfy the requirements of lower cost and higher production efficiency, simple raw materials and effective processes are required. Consequently, the synthesis of dielectric materials must be simplified without degrading their microwave dielectric properties [13–15].

$CaTiO_3$ is a typical orthogonally distorted perovskite with dielectric constant (ε_r) ≈ 170, quality factor ($Q \times f$) ≈ 3600 GHz, and resonance frequency temperature coefficient (τ_f) ≈ 800 ppm/°C [16]. Because it has a large positive τ_f value, it acts as a regulator to control the microwave dielectric properties of other materials. For example, the addition of $CaTiO_3$ could lead to the formation of a solid solution with $SmAlO_3$ (ε_r = 20.4, Q ≈ 6500, τ_f ≈ −74 ppm/°C) and the adjustment of the properties of the resulting ceramics. $CaTiO_3$-$SmAlO_3$ solid solution ceramics have a large ε_r (≈40–47), high $Q \times f$ (≈40 000 GHz), and near-zero τ_f; hence, they are ideal candidate materials for microwave applications [17–20]. Using $SmAlO_3$ powders as raw materials synthesized via the co-precipitation method, the sintering temperature of 0.7 $CaTiO_3$-0.3$SmAlO_3$ could be reduced to 1410 °C. The ceramics also showed improved microwave dielectric performance, with ε_r = 44.95, $Q \times f$ = 50 137 GHz, and τ_f = +7.6 ppm/°C [21]. As well known, CeO_2 exhibited good microwave dielectric properties with ε_r = 24, $Q\times f$ = 57 000, τ_f = −104 ppm/°C and was used as dopant to imropve the properties of other

* Corresponding author.
E-mail address: zhouhuanfu@163.com (H. Zhou).

https://doi.org/10.1016/j.ceramint.2020.09.231
Received 21 August 2020; Received in revised form 22 September 2020; Accepted 24 September 2020
Available online 25 September 2020

materials system. Bhuyan et al. reported that the addition of 1.5 wt% CeO_2 improved the microwave dielectric performance of Mg_2TiO_4 ceramic to $\varepsilon_r = 14.6$ and $Q\times f = 167\ 000$ GHz [22]. In this study, CeO_2-doped CTSA ceramics were synthesized using the RS process to simplify the sintering process and enhance the dielectric properties. In addition, the sintering behavior, microstructure, phase formation, and dielectric performance of CTSA solid solution ceramics were studied [23,24].

2. Materials and methods

$CaTiO_3$-$SmAlO_3$ ceramic samples were synthesized via the RS method using $CaCO_3$ (≥99%, Sinopharm Chemical Reagent, China), TiO_2 (≥99%, Xiantao Zhongxing, China), Al_2O_3 (≥99.2%, Sinopharm Chemical Reagent, China), Sm_2O_3 (≥99.99%, Sinopharm Chemical Reagent, China), and CeO_2 (≥99%, Sinopharm Chemical Reagent, China). The mole ratio of $CaTiO_3$-$SmAlO_3$ was determined to be 0.695:0.305 in this study, while various contents (0–1.5 wt%) of CeO_2 were used as additives. To prevent the rare earth oxides to absorb the moisture and carbon dioxide from the air. Sm_2O_3 and CeO_2 were preheated at 900 °C for 2 h before weighing. The powders were mixed with zirconia balls in an ethanol medium for 4 h and dried in an oven. Thereafter, the dried mixed powders were pressed to a diameter of 10 mm and cylinder height of 5 mm at 10 MPa. Finally, the cylinders were directly sintered at 1450–1550 °C for 6 h.

The crystalline structure of the sintered ceramics was investigated via X-ray diffraction (Model X'Pert PRO, PANalytical, Almelo, Holland) with Cu K_α radiation at 40 kV and 40 mA ($5° \le 2\theta \le 80°$). The morphology and grain growth were investigated using scanning electron microscopy (Model JSM6380-LV SEM, JEOL, Tokyo, Japan). Microwave dielectric performances of specimens were analyzed using a network analyzer (Model E5071 CENA, Agilent Co, California, USA, 300 KHz-20GHz). The τ_f values of the samples were calculated from the resonant frequencies at 25–85 °C, in accordance with the following formula:

$$\tau_f = (f_T - f_0)/f_0(T - T_0) \quad (1)$$

where f_T and f_0 are the resonance frequencies at 85 and 25 °C, respectively.

3. Results and discussion

Fig. 1 shows the XRD patterns of 0.695$CaTiO_3$-0.305$SmAlO_3$+$x$wt% CeO_2 (x = 0, 0.5, 1.0, 1.5) ceramics synthesized through the RS method. Upon heating at 1100 °C, the ceramic samples contained both $CaTiO_3$ and $SmAlO_3$ phases. When the temperature increased to 1200 °C, the major peak of the CTSA ceramic occurred at $2\theta = 33.3°$, which is a good match with the 2θ value of the $CaTiO_3$ phase. All the diffraction peaks show a uniform main phase of $CaTiO_3$, corresponding to the orthorhombic perovskite structure (PDF: 01-075-0437) and belonging to the Pbnm space group. In order to determine the cation occupation of the samples, the XRD pattern of the 0.695$CaTiO_3$-0.305$SmAlO_3$+0.5 wt% CeO_2 ceramic sintered at 1500 °C was refined using the GSAS software, the Rietveld refinement is demonstrated in Fig. 2. The samples exhibit a single $CaTiO_3$ phase with a typical perovskite structure, and the lattice constants are as follows: a = 5.358072 (6)Å, b = 7.593186 (10) Å, c = 5.394203 (5) Å, and $\alpha = \beta = \gamma = 90°$. The small R-values ($Rp$ = 3.07%, Rwp = 4.37%) indicate that the XRD result is consistent with $CaTiO_3$ (PDF: 01-075-0437) with an orthorhombic structure [25]. The refinement parameters are listed in Table 1. The crystalline properties of the ceramics changed as the sintering temperature increased. This shows that CeO_2 is integrated into 0.695$CaTiO_3$-0.305$SmAlO_3$ ceramics, and a solid solution is completely formed. Ca^{2+}, Sm^{3+}, and Ce^{4+} occupy the A site of the oxygen octahedron, while Ti^{4+} and Al^{3+} occupy the B site of the oxygen octahedron [26,27].

Fig. 3 illustrates the SEM images and grain size of 0.695$CaTiO_3$-0.305$SmAlO_3$+$x$wt% CeO_2 (x = 0, 0.5, 1.0, 1.5) ceramics sintered at 1500 °C for 6 h. With regard to the ceramic sample without CeO_2, the microstructure of the ceramic is very rough, the size distribution is uneven, and the grain growth is asymmetrical, thereby resulting in high porosity and low bulk density [28], as shown in Fig. 3(a). Upon doping with CeO_2, the porosity of CTSA ceramics decreased, accompanied by an increase in the homogeneity of the grains. The average grain size of the 0.5 wt% CeO_2 sample declined sharply, and the average particle size was 7.34 μm. When the CeO_2 content was increased to 1.5 wt%, there were some obvious pores and the grain growth of the sample was abnormal. In addition, with an excessive addition of CeO_2, aberrant grain growth and high porosity will degrade the dielectric performance of CTSA ceramics [29,30].

Fig. 4 shows the curve of the bulk density of the ceramics versus the sintering temperature. The bulk densities of 0, 0.5, 1.0, and 1.5 wt% CeO_2-doped ceramics were 4.59–4.70 g/cm^3, 4.64–4.93 g/cm^3, 4.66–4.78 g/cm^3, and 4.51–4.61 g/cm^3, respectively. The bulk density increased with increasing sintering temperature due to the pore discharge and grain growth in the sintering process of the ceramic, reaching a maximum value at 1500 °C. When the CeO_2 content was 0.5

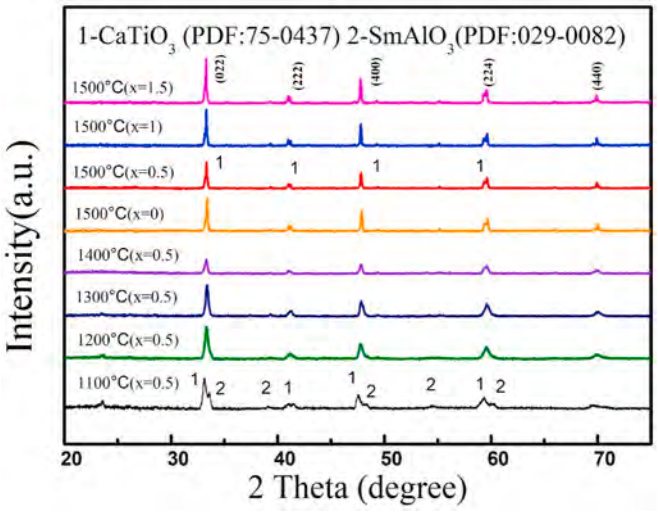

Fig. 1. XRD patterns of 0.695$CaTiO_3$-0.305$SmAlO_3$+$x$wt% CeO_2(x = 0, 0.5, 1.0, 1.5) ceramics sintered at different temperatures.

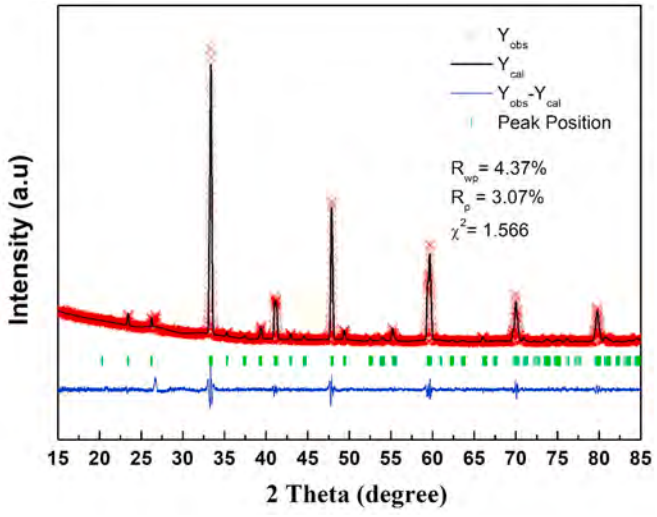

Fig. 2. Rietveld refinement of the room temperature XRD patterns of 0.695$CaTiO_3$-0.305$SmAlO_3$+0.5 wt% CeO_2 ceramic sintered at 1500 °C (R_{wp} = 4.37%, R_p = 3.07%, χ^2 = 1.566).

Table 1
Refinement parameters of $0.695CaTiO_3$-$0.305SmAlO_3$+0.5 wt% CeO_2 ceramic sintered at 1500 °C.

CTSA	a	b	c	α	β	γ	Vol (Å^3)
	5.3588	7.5916	5.3934	90.0000	90.0000	90.0000	219.426
	x		y		z		Occupancy
Ca/Sm	0.0000		0.2500		0.0300		1
Ti/Al	0.5000		0.0000		0.0000		1
O1	0.4630		0.2500		−0.0180		1
O2	0.2320		−0.0260		0.2320		1

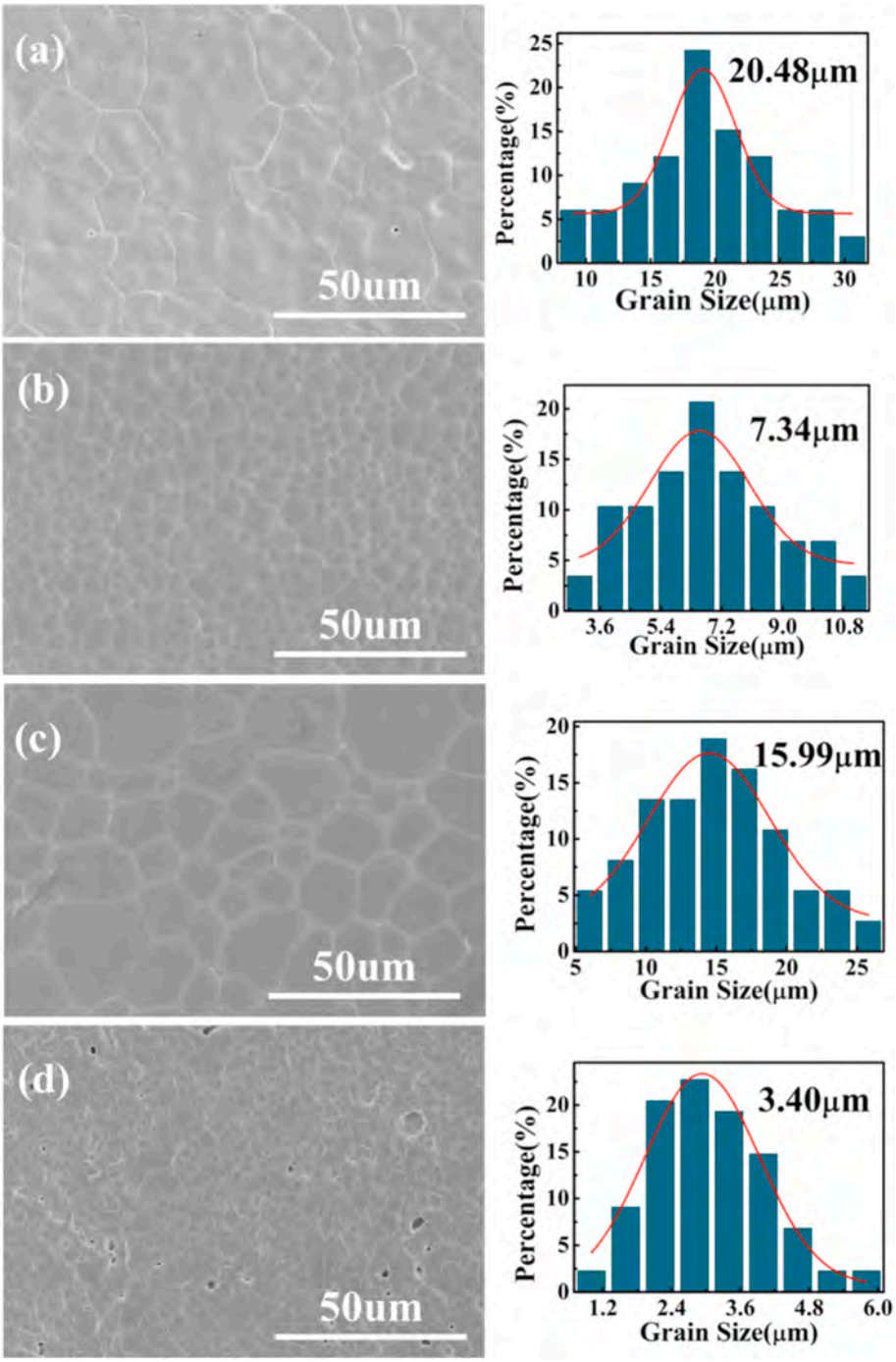

Fig. 3. SEM images and grain size of $0.695CaTiO_3$-$0.305SmAlO_3$+$x$wt%CeO_2(x = 0, 0.5, 1.0, 1.5) ceramics at 1500 °C for 6 h.

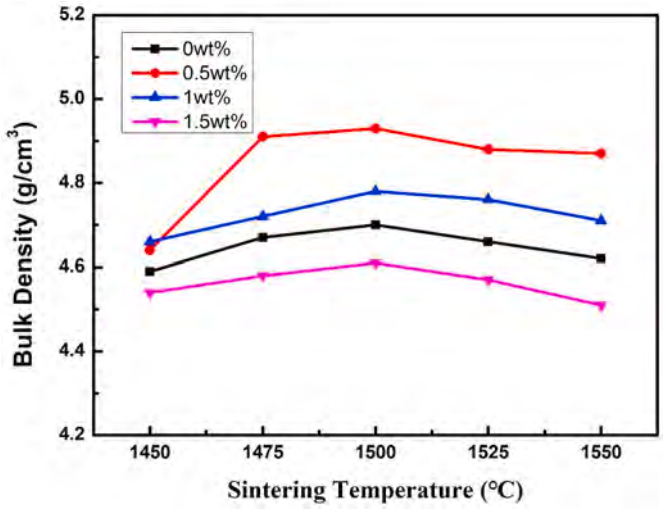

Fig. 4. The bulk densities (g/cm^3) of 0.695$CaTiO_3$-0.305$SmAlO_3$+$x$wt% CeO_2 (x = 0, 0.5, 1.0, 1.5) ceramics at different temperatures.

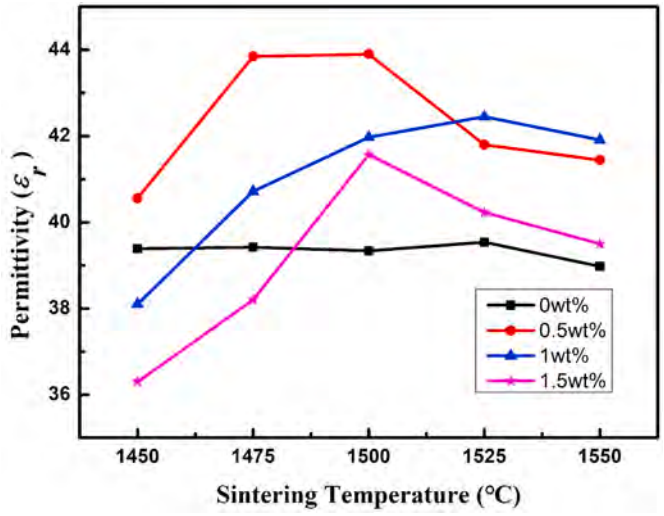

Fig. 5. The dielectric constants of 0.695$CaTiO_3$-0.305$SmAlO_3$+$x$wt% CeO_2 (x = 0, 0.5, 1.0, 1.5) ceramics at different temperatures.

wt%, the ceramic exhibited optimal bulk density, thereby showing that the appropriate CeO_2 addition could promote the sintering behavior of $CaTiO_3$-$SmAlO_3$ ceramics. A comparison of $CaTiO_3$-$SmAlO_3$ ceramics prepared through different processes is listed in Table 2. Due to the over-sintering phenomenon of ceramics at sintering temperatures above 1500 °C, the grain growth rate was excessively fast and the pores could not be discharged in time. Therefore, the abnormal grain growth phenomenon led to a decrease in the density of CTSA ceramics [31].

Fig. 5 illustrates the permittivity of 0.695$CaTiO_3$-0.305$SmAlO_3$+$x$wt % CeO_2 (x = 0, 0.5, 1.0, 1.5) ceramics at different sintering temperatures. When the x value changed from 0 to 0.5, the permittivity of CTSA ceramics rose from 39.5 to 43.9. For values of x greater than 0.5, the permittivity of ceramics decreased with a further increase in the x value. It is clear that the proper CeO_2 dopant level could improve the permittivity in 0.695$CaTiO_3$-0.305$SmAlO_3$ ceramics. During the sintering process of ceramics, the growth of crystal grains discharges the pores in the ceramics, which densifies the ceramics [32]. The increase in bulk density increases the number of polarized particles per unit volume, thereby increasing the polarization rate between ions, which consequently increases the permittivity of the ceramic [33]. When the sintering temperature exceeds 1500 °C, the over-sintering phenomenon occurs, which induces the inability to discharge the pores in time, abnormal growth of the crystal grains, and a decrease in the compactness of the ceramic, thereby resulting in a decrease in permittivity [16]. As the concentration of additives increases, the reduction in permittivity is mainly attributed to the decrease in bulk density and the substitution of ions [34]. Ce^{4+} (0.87 Å) has a larger ionic radius than Ti^{4+} (0.605 Å), which causes a distortion of the BO_6 octahedron. Under the action of an external electric field, small ions move easily in the BO_6 octahedron. The decrease in the large ion mobility gives rise to the reduction in permittivity [35].

Fig. 6 shows how the $Q \times f$ values of CTSA ceramics with different

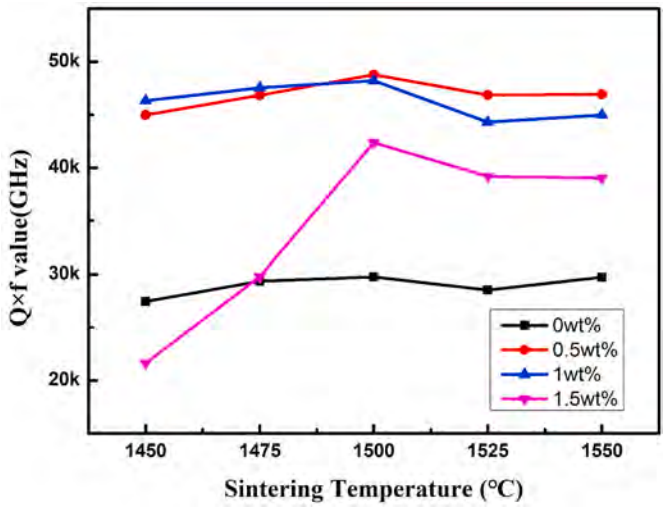

Fig. 6. The quality factors of 0.695$CaTiO_3$-0.305$SmAlO_3$+$x$wt% CeO_2 (x = 0, 0.5, 1.0, 1.5) ceramics at different temperatures.

CeO_2 content change with temperature. The $Q \times f$ values of 0.695$CaTiO_3$-0.305$SmAlO_3$+$x$wt% CeO_2 (x = 0, 0.5, 1.0, 1.5) ceramics vary from 21 635 to 48 779 GHz over the range of 1450–1550 °C. The maximal $Q \times f$ value of 48 779 GHz was obtained for an addition of 0.5 wt% CeO_2 at 1500 °C. Furthermore, it is clearly seen that the $Q \times f$ value presents the trend of increasing first and then decreasing with doping CeO_2 content [36]. The substitution of Ce^{4+} for Ti^{4+} could be non-stoichiometric, with some Ti vacancies in the CTSA ceramics [26].

The variation in the temperature coefficients of the resonant frequency of 0.695$CaTiO_3$-0.305$SmAlO_3$+$x$wt% CeO_2 (x = 0, 0.5, 1.0, 1.5) ceramics with temperature are shown in Fig. 7. Excellent thermal stability is ideal for applications regarding ceramics. Considering the same phase of $CaTiO_3$-$SmAlO_3$ in all samples sintered at a temperature range of 1450–1550 °C, the fluctuations of τ_f value are mainly due to grain size, porosity, oxygen vacancies, and the like [37]. All ceramics exhibited a small τ_f value. In particular, the 0.695$CaTiO_3$-0.305$SmAlO_3$+0.5 wt% CeO_2 ceramic sintered at 1500 °C for 6 h had a near-zero τ_f value of −0.24 ppm/°C. Due to the large negative τ_f value (τ_f = −104 ppm/°C) of CeO_2, the τ_f value of 0.695$CaTiO_3$-0.305$SmAlO_3$ ceramics decreased with increasing the content of CeO_2.

Table 2
Microwave dielectric properties of $CaTiO_3$-$SmAlO_3$ ceramics prepared by different methods.

Sintering method	ρ (g/cm^3)	$Q \times f$ (GHz)	ε_r	τ_f (ppm/°C)
RS method (CeO_2)	4.93	48 779	43.9	−0.24
Solid reaction method (CeO_2)	4.98	45 348	44.05	−0.48
Solid reaction method (ZrO_2 and ZnO) [26]	4.85	38 600	44.65	−8.36
Co-precipitation method [16]	4.81	50 137	44.95	+7.6

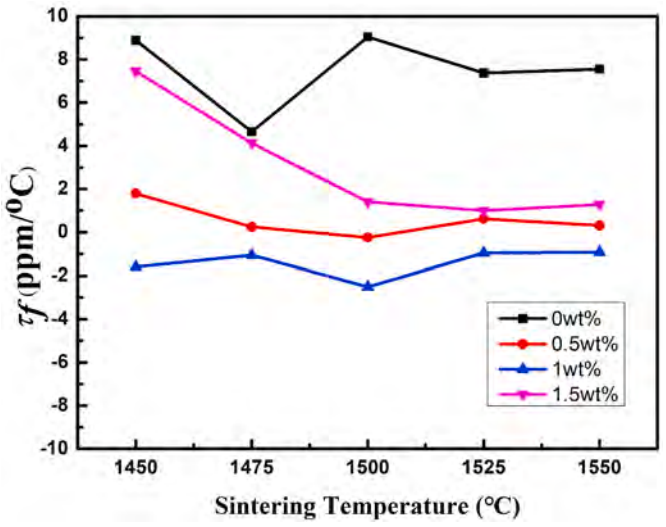

Fig. 7. The temperature coefficients of resonance frequency of $0.695CaTiO_3$-$0.305SmAlO_3$+$x$wt% CeO_2 (x = 0, 0.5, 1.0, 1.5) ceramics at different temperatures.

4. Conclusion

$0.695CaTiO_3$-$0.305SmAlO_3$+$x$wt% CeO_2 (x = 0, 0.5, 1.0, 1.5) ceramics were synthesized through the RS route. Doping with CeO_2 improved the microstructure and dielectric performance of CTSA ceramics. The bulk density of 0.5 wt% CeO_2-doped CTSA ceramics sintered at 1500 °C for 6 h exhibited the maximum value of 4.93 g/cm^3. This ceramic exhibited optimized microwave dielectric properties of $Q \times f =$ 48 779 GHz, ε_r = 43.9, and τ_f = −0.24 ppm/°C. Compared with the traditional two-step solid-state reaction method, the reaction sintering method requires only one step, which simplifies the preparation procedure and reduces the preparation cost, thereby indicating that RS is a simple method for preparing CTSA ceramics.

Declaration of competing interest

The authors declare that they have no known competing financial interests or personal relationships that could have appeared to influence the work reported in this paper.

Acknowledgment

This work was supported by the Natural Science Foundation of China (Nos. 61761015 and 11664008) and the Natural Science Foundation of Guangxi (Nos. 2017GXNSFFA198011, 2018GXNSFFA050001, and 2017GXNSFDA198027) and High Level Innovation Team and Outstanding Scholar Program of Guangxi Institutes.

References

[1] H.F. Zhou, W.D. Sun, X.B. Liu, K.G. Wang, H. RuanX, L. Chen, Microwave dielectric properties of $LiCa_3ZnV_3O_{12}$ and $NaCa_2Mg_2V_3O_{12}$ ceramics prepared by reaction-sintering, Ceram. Int. 45 (2) (2019) 2629–2634.
[2] H.T. Yu, T. Luo, L. HeJ, S. Liu, Effect of ZnO on Mg_2TiO_4-$MgTiO_3$-$CaTiO_3$ microwave dielectric ceramics prepared by reaction sintering route, Adv. Appl. Ceram. 118 (3) (2019) 98–105.
[3] C.F. Xing, Y.H. Zhang, B.J. Tao, H.T. WuY, Y. Zhou, Crystal structure, infrared spectra and microwave dielectric properties of low-firing $La_2Zr_3(MoO_4)_{(9)}$ ceramics prepared by reaction-sintering process, Ceram. Int. 45 (17) (2019) 22376–22382.
[4] G. Wang, D.N. Zhang, G.W. Gan, Y. Yang, Y.H. Rao, F. Xu, X. Huang, Y.L. Liao, J. Li, C. Liu, L.C. JinH, W. Zhang, Synthesis, crystal structure and low loss of $Li_3Mg_2NbO_6$ ceramics by reaction sintering process, Ceram. Int. 45 (16) (2019) 19766–19770.
[5] L. He, H.T. Yu, M.S. Zeng, E.Z. Li, J.S. LiuS, R. Zhang, Phase compositions and microwave dielectric properties of $MgTiO_3$-based ceramics obtained by reaction-sintering method, J. Electroceram. 40 (4) (2018) 360–364.
[6] X.L. Chen, H.F. Zhou, L.A. Fang, X.B. LiuY, L. Wang, Microwave dielectric properties and its compatibility with silver electrode of $Li_2MgTi_3O_8$ ceramics, J. Alloys Compd. 509 (19) (2011) 5829–5832.
[7] H.F. Zhou, X.B. Liu, X.L. Chen, L. FangY, L. Wang, $ZnLi_{2/3}Ti_{4/3}O_4$: a new low loss spinel microwave dielectric ceramic, J. Eur. Ceram. Soc. 32 (2) (2012) 261–265.
[8] C.J. Pei, X.S. Hu, G.G. YaoH, Q. Yang, Reaction-sintering method for microwave dielectric $Li_2CoTi_3O_8$ ceramic, Ferroelectrics 505 (1) (2016) 4–9.
[9] H.B. Bafrooei, E.T. Nassaj, T. Ebadzadeh, C.F. Hu, A. Sayyadi-Shahraki, T. Kolodiazhnyi, Sintering behavior and microwave dielectric characteristics of $ZnTiNb_2O_8$ ceramics achieved by reaction sintering of ZnO-TiO_2-Nb_2O_5 nanosized powders, Ceram. Int. 42 (2) (2016) 3296–3303.
[10] G.G. Yao, Synthesis and microwave dielectric properties of $Li_2ZnTi_3O_8$ ceramics by the reaction-sintering process, J. Ceram. Process. Res. 16 (1) (2015) 41–44.
[11] H.F. Zhou, X.H. Tan, J. Huang, N. Wang, G.C. FanX, L. Chen, Phase structure, sintering behavior and adjustable microwave dielectric properties of $Mg_{1-x}Li_{2x}Ti_xO_{1+2x}$ solid solution ceramics, J. Alloys Compd. 696 (2017) 1255–1259.
[12] W.T. Xie, Q.X. Jiang, Q.L. Cao, H.Q. Zhou, L.C. RenX, F. Luo, Microwave dielectric properties of (1-x)$ZnNb_2O_6$-xBa($Zn_{1/3}Nb_{2/3}$)O_3 compound ceramic with near zero temperature coefficient, J. Mater. Sci. Mater. Electron. 29 (3) (2018) 2170–2174.
[13] J.M. Li, P. Xu, T. QiuL, C. Yao, Sintering characteristics and microwave dielectric properties of $0.5Ca_{(0.6)}La_{(0.267)}TiO_{(3)}$-$0.5Ca(Mg_{1/3}Nb_{2/3})O_3$ ceramics prepared by reaction-sintering process, J. Rare Earths 36 (4) (2018) 404–408.
[14] J.D. Guo, W.B. Ma, M.J. Ma, H.D. Zhao, Y.X. YangJ, F. Gao, Sintering characteristic and microwave dielectric properties of ultra-low loss $Li_2Mg_3TiO_6$ ceramic prepared by reaction-sintering process, J. Mater. Sci. Mater. Electron. 29 (5) (2018) 3640–3647.
[15] W.C. Tsai, K.C. Chiu, Y.X. NianY, C. Liou, Significant improvement of the microwave dielectric loss of $Zn_{1.95}M_{0.05}SiO_4$ ceramics (M = Zn, Mg, Ni, and Co) prepared by reaction-sintering process, J. Mater. Sci. Mater. Electron. 28 (19) (2017) 14258–14263.
[16] Z.H. Qin, Y.F. Huang, C.Y. ShenM, L. Tang, Effect of preparation method on microwave dielectric properties of $0.7CaTiO_3$-$0.3SmAlO_3$ ceramic, J. Mater. Sci. Mater. Electron. 27 (4) (2016) 4157–4162.
[17] H.H. Guo, D. Zhou, C. Du, P.J. Wang, W.F. Liu, L.X. Pang, Q.P. Wang, J.Z. Su, C. Singh, S. Trukhanov, Temperature stable $Li_2Ti_{0.75}(Mg_{1/3}Nb_{2/3})_{(0.25)}O_3$-based microwave dielectric ceramics with low sintering temperature and ultra -low dielectric loss for dielectric resonator antenna applications, J. Mater. Chem. C. 8 (14) (2020) 4690–4700.
[18] X.Q. Song, W. Lei, Y.Y. Zhou, T. Chen, S.W. Ta, Z.X. FuW, Z. Lu, Ultra-low fired fluoride composite microwave dielectric ceramics and their application for $BaCuSi_2O_6$-based LTCC, J. Am. Ceram. Soc. 103 (2) (2020) 1140–1148.
[19] Z.Y. Tan, K.X. Song, H.B. Bafrooei, B. Liu, J. Wu, J.M. Xu, H.X. LinD, W. Wang, The effects of TiO2 addition on microwave dielectric properties of $Y_3MgAl_3SiO_{12}$ ceramic for 5G application, Ceram. Int. 46 (10) (2020) 15665–15669.
[20] K.G. Wang, H.F. Zhou, X.B. Liu, W.D. Sun, X.L. Chen, H. Ruan, A lithium aluminium borate composite microwave dielectric ceramic with low permittivity, near-zero shrinkage, and low sintering temperature, J. Eur. Ceram. Soc. 39 (4) (2019) 1122–1126.
[21] T. Yang, Z.X. Han, P. LiuB, C. Guo, Microwave dielectric properties of $Mg_4Nb_2O_9$ ceramics with excess $Mg(OH)_2$ produced by a reaction-sintering process, Ceram. Int. 41 (2015) S572–S575.
[22] R.K. Bhuyan, T.S. Kumar, D. Goswami, A.R. James, A. Perumal, D. Pamu, Enhanced densification and microwave dielectric properties of Mg_2TiO_4 ceramics added with CeO_2 nanoparticles, Mater. Sci. Eng. B-Adv. Funct. Solid-State Mater. 178 (7) (2013) 471–476.
[23] S. Seidel, C. Patzig, M. Krause, T. Hoche, A. Gawronski, Y.F. Hu, C. Russel, The effect of CeO_2 on the crystallization of MgO-Al_2O_3-SiO_2-ZrO_2 glass, Mater. Chem. Phys. 212 (2018) 60–68.
[24] K.G. Wang, T.T. Yin, H.F. Zhou, X.B. Liu, J.J. Deng, S.X. Li, C.M. LuX, L. Chen, Bismuth borate composite microwave ceramics synthesised by different ratios of H_3BO_3 for ULTCC technology, J. Eur. Ceram. Soc. 40 (2) (2020) 381–385.
[25] Z.Y. Zou, Z.H. Chen, X.K. Lan, W.Z. Lu, B. Ullah, X.H. Wang, W. Lei, Weak ferroelectricity and low-permittivity microwave dielectric properties of $Ba_2Zn_{(1+x)}Si_2O_{(7+x)}$ ceramics, J. Eur. Ceram. Soc. 37 (9) (2017) 3065–3071.
[26] L.S. Hu, H.Q. Zhou, Q.L. Sun, L.C. Ren, X.F. Luo, Y.K. HuY, S. Xia, Effects of ZrO_2-ZnO on the sintering behavior and microwave dielectric properties of $0.65CaTiO_3$-$0.35SmAlO_3$ ceramics, J. Mater. Sci. Mater. Electron. 27 (12) (2016) 12834–12839.
[27] Y.C. Liou, S.L. YangS, Y. Chu, Effects of MgO and $Mg(OH)_2$ on phase formation and properties of $MgTiO_3$ microwave dielectric ceramics, J. Electron. Mater. 44 (4) (2015) 1062–1070.
[28] M.R. VarmaN, D. Kataria, Effect of dopants on the low temperature microwave dielectric properties of Ba($Zn_{1/3}Ta_{2/3}$)O_3 ceramics, J. Mater. Sci. Mater. Electron. 18 (4) (2007) 441–446.
[29] G. Wang, J. Jiang, Z.M. Dou, F. ZhangT, J. Zhang, Sintering behavior and microwave dielectric properties of $0.67CaTiO_{(3)}$-$0.33LaAlO_{(3)}$ ceramics modified by B_2O_3-Li_2O-Al_2O_3 and CeO_2, Ceram. Int. 42 (9) (2016) 11003–11009.
[30] M. Bari, E. Taheri-Nassaj, H. Taghipour-Armaki, Phase evolution, microstructure, and microwave dielectric properties of reaction-sintered $Li_2ZnTi_3O_8$ ceramic obtained using nanosized TiO_2 reagent, J. Electron. Mater. 44 (10) (2015) 3670–3676.
[31] T. Luo, Q.H. Yang, H.T. YuJ, S. Liu, Formation mechanism and microstructure evolution of $Ba_2Ti_9O_{20}$ ceramics by reaction sintering method, J. Am. Ceram. Soc. 103 (2) (2020) 1079–1087.
[32] I.N. Lin, C.-B. Chang, K.-C. Leou, H.-F. Cheng, Effect of reaction sintering process on the microwave dielectric properties of $Ba_2Ti_9O_{20}$ materials, J. Eur. Ceram. Soc. 30 (2) (2010) 159–163.

[33] H.J. Hu, C.E. Huang, J. Nan, H. WangC, Y. Shen, Effects of co-precipitation method on microwave dielectric properties of $0.7CaTiO_3$-$0.3SmAlO_3$ ceramics, Mater. Res. Express 7 (1) (2020), 2053-1591.
[34] W.T. Xie, Q.X. Jiang, Q.L. Cao, Q.L. ChenH, Q. Zhou, Effect of cooling rate on microstructure and microwave dielectric properties of MgO doped $(Sr,Ca)TiO_3$-$(Sm,Nd)AlO_3$ ceramics, J. Mater. Sci. Mater. Electron. 28 (9) (2017) 6407–6412.
[35] L.M. Zhang, Y. Chang, M. Xin, X.F. Luo, H.J. Tao, Y. Fu, P.Z. LiH, Q. Zhou, Synthesis of $0.65CaTiO_{(3)}$-$0.35SmAlO_{(3)}$ ceramics and effects of La_2O_3/SrO doping on their microwave dielectric properties, J. Mater. Sci. Mater. Electron. 29 (24) (2018) 21205–21212.
[36] A. Sayyadi-Shahraki, E. Taheri-Nassaj, H. Barzegar-BafrooeiS, A. Hassanzadeh-Tabrizi, Microwave dielectric properties of $Li_2ZnTi_3O_8$ ceramics prepared by reaction-sintering process, J. Mater. Sci. Mater. Electron. 25 (2) (2014) 1117–1121.
[37] X.P. Lu, Y. Zheng, Z.W. Dong, W.Y. Zhang, Q. Huang, Microstructures and microwave dielectric properties of $Li_2ZnTi_3O_8$ ceramics prepared by reaction-sintering process, J. Mater. Sci. Mater. Electron. 25 (8) (2014) 3358–3363.